



Fuzzy scheduling of robust controllers for islanded DC microgrids applications

Giacomo Canciello¹ · Alberto Cavallo¹ · Michele Cucuzzella² · Antonella Ferrara³

Received: 12 March 2018 / Revised: 12 December 2018 / Accepted: 18 December 2018 / Published online: 3 January 2019
© Springer-Verlag GmbH Germany, part of Springer Nature 2019

Abstract

In the present paper a decentralized control scheme that relies on sliding mode (SM) and high gain control methodologies to regulate the load voltage in buck-based islanded direct current (DC) microgrids is designed. First, the model of a buck-based islanded DC microgrid consisting of several Distributed Generation units interconnected through an arbitrary complex and meshed topology including rings is introduced. More precisely, the topology of the power network is represented by its corresponding incidence matrix, and in the model the power lines dynamics is considered. Moreover, it is assumed that the microgrid is affected by unknown load demand and unavoidable modelling uncertainties. A mixed strategy, employing both a third-order sliding mode (3-SM) control algorithm and a high gain control strategy, with a fuzzy scheduling is designed to solve the voltage control problem in a decentralized manner. Specifically, the high-gain control reduces the stress on the generator during abrupt reference changes, the 3-SM guarantees finite-time voltage regulation and strong robustness with respect to load variations. Fuzzy scheduling merges the two strategies. Finally, detailed simulation results confirm the effectiveness of the proposed control strategy.

Keywords Sliding mode control · High gain control · DC microgrid · Fuzzy scheduling

1 Introduction

In the last decades several economic, technological and environmental aspects have inspired and motivated the transformation of the traditional power generation and transmission towards smaller and renewable Distributed Generation units (DGus) [1–3]. However, the increasing penetration of

the Renewable Energy Sources (RES), such as photovoltaic arrays or wind turbines, due to the unpredictable generation, has given rise to a new challenge for operating and controlling the power network safely and efficiently [4,5]. This challenge has been recently faced by exploiting the so-called “microgrids”, which are clusters of DGus, loads and storage systems interconnected through power lines [6–10]. Moreover, they can also operate autonomously, i.e., disconnected from the main grid, in the so-called islanded operation mode [11,12].

In this context, due to the traditional widespread use of Alternate Current (AC) electricity in the majority of industrial, commercial and residential applications, the research mainly focused on developing control solutions for AC microgrids [13–17]. However, the fast technological development in power electronics, and the increasing number of DC loads in several fields (e.g. automotive [18], marine, avionics [19–22]), recently moved the interest to DC microgrids [23]. More precisely, several aspects, in terms of efficiency, encourage the use of DC-based power systems: (i) RESs and fuel cells generate DC electricity, (ii) only the active power needs to be controlled, (iii) the notorious skin

✉ Giacomo Canciello
gcanciello@gmail.com

Alberto Cavallo
alberto.cavallo@unicampania.it

Michele Cucuzzella
m.cucuzzella@rug.nl

Antonella Ferrara
antonella.ferrara@unipv.it

¹ Dipartimento di Ingegneria Industriale e dell’Informazione, University of Campania “L. Vanvitelli”, via Roma 29, 81031 Aversa, Italy

² ENTEG, University of Groningen, Nijenborgh 4, 9747 AG Groningen, Netherlands

³ Dipartimento di Ingegneria Industriale e dell’Informazione, University of Pavia, via Ferrata 5, 27100 Pavia, Italy

effect is avoided, (iv) power lossy DC–AC and AC–DC conversion stages are reduced [24,25].

In the literature, the problem of control the voltage in DC microgrids has been studied and solved with different control approaches (see for instance [26–28] and the references therein). In [29–31] consensus algorithms are designed in order to perform power sharing between the DGus of the microgrid. A genuine fuzzy control strategy is designed in [32], while [33] uses fuzzy methodology together with gain-scheduling techniques to accomplish both current sharing and energy management. Instead in [34] a droop current controller is proposed to interface photovoltaic arrays with DC distribution power grids, and a model predictive controller is designed to track the maximum power point.

In this paper an islanded DC microgrid with DGus interconnected according to an arbitrary complex and meshed topology including rings is considered, and each DGU is interfaced with the network through a DC–DC Buck converter. The power network topology is represented by a connected and undirected graph, and the model, that takes into account the power lines dynamics, is affected by unknown load demand and unavoidable modelling uncertainties.

The proposed solution relies on the Sliding Mode (SM) control methodology. SM control belongs to the class of Variable Structure Control Systems so that it seems perfectly adequate to control the variable structure nature of DC–DC converters even in presence of unavoidable modelling uncertainties and external disturbances [35–39]. More precisely, a second order sliding mode control algorithm [40] could be designed to solve the aforementioned voltage control problem. However, this solution allows the switching frequency of the Buck converter to be not constant and not a priori fixed. So, the switching frequency could be very high, implying the increase of the power losses. Then, in order to avoid this problem and obtain a continuous control signal that can be used as duty cycle of the Buck converter, a third order Sliding Mode (3-SM) control [41] is proposed together with a Levant’s second order differentiator [42]. In fact, we assume that only the load voltage can be locally measured. This makes the proposed control approach decentralized and easy to implement.

Another possibility is to implement second-order sliding manifold strategies by using a high-gain control approach [43–45]. Making reference to [46,47], the sliding manifold is initially “bent” so that the initial state of the controlled system lies since the beginning on the sliding surface, thus avoiding any reaching phase. The bending is controlled by an exponentially decaying term. Once the exponential action is negligible, the high gain control allows to stay close to the original, unbent, manifold thus bringing the error to small values. Robustness with respect to unknown disturbances and uncertain parameters is moreover assured by high gain control [48]. Note however that, while the sliding mode control assures finite-time reaching of the sliding surface, the high

gain strategy can only guarantee asymptotic reaching. On the other side, control action is limited since the beginning with the high-gain control, while nothing can be said about the third-order sliding mode during the reaching phase.

Motivated by the above considerations, we propose in this paper a mixed strategy, employing both a third-order sliding mode controller and a high-gain controller in the reaching phase, with a fuzzy scheduler to select, or better, to combine the two strategies. Finally, the proposed solutions are theoretically analyzed and assessed in simulation.

The present paper is organized as follows: Sect. 2 introduces the microgrid model together with some basic notions on DGus, while in Sect. 3 the control problem is formulated. The proposed control scheme is presented in Sect. 4. In Sect. 5 the simulation results are illustrated and discussed. Some conclusions are gathered in Sect. 6.

2 Microgrid model

In this section, for the readers’ convenience, some basic notions on DGus are discussed. Then, the dynamic model of a microgrid is presented.

$$A = \begin{bmatrix} -L_t^{-1}R_t & -L_t^{-1} & 0_{n \times m} \\ C_t^{-1} & 0_{n \times n} & C_t^{-1}\mathcal{B} \\ 0_{m \times n} & -L^{-1}\mathcal{B}^T & -L^{-1}R \end{bmatrix}, \quad B = \begin{bmatrix} L_t^{-1} \\ 0_{n \times n} \\ 0_{m \times n} \end{bmatrix},$$

$$B_w = \begin{bmatrix} 0_{n \times n} \\ -C_t^{-1} \\ 0_{m \times n} \end{bmatrix}, \quad C = [0_{n \times n} \quad I_{n \times n} \quad 0_{n \times m}].$$

In Fig. 1 the schematic electrical diagram of a typical microgrid composed of two DGus is reported. The renewable energy source (e.g. photovoltaic panels) of a DGU is represented by a direct current (DC) voltage source V_{DC} which is interfaced with the electric DC network through a DC–DC Buck converter. The latter feeds a local DC load, which is connected to the so-called Point of Common Coupling (PCC), and it can be treated as a current disturbance W . At the output of the Buck converter, a low-pass filter $R_t L_t C_t$ is considered, where R_t represents the filter parasitic resistance. Moreover, the DGU_{*i*} can exchange power with the DGU_{*j*} through the resistive-inductive interconnecting line $R_{ij} L_{ij}$.

Now, the dynamic model of a microgrid composed of n DGus is presented.¹ The power network is represented by a connected and undirected graph $\mathcal{G} = (\mathcal{V}, \mathcal{E})$, where the nodes $\mathcal{V} = \{1, \dots, n\}$, represent the DGus and the edges $\mathcal{E} \subset \mathcal{V} \times \mathcal{V} = \{1, \dots, m\}$, represent the distribution power lines interconnecting the DGus. First, consider the model of a microgrid composed of two DGus as reported in Fig. 1.

¹ For the sake of simplicity, the dependence of all the variables on time t is omitted throughout the paper.

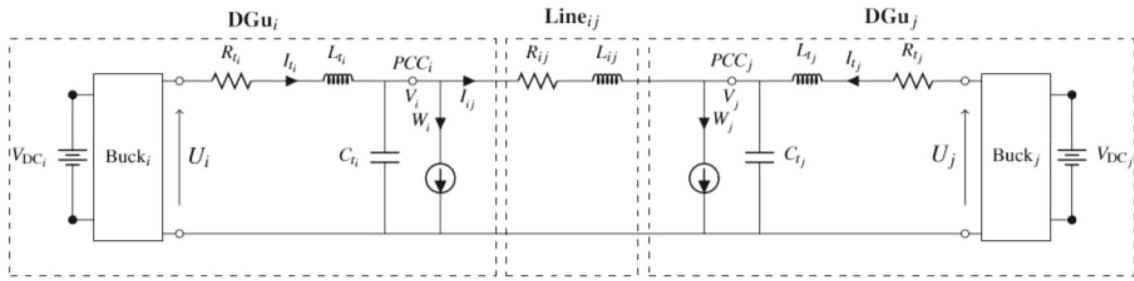


Fig. 1 The considered electrical diagram of a typical DC microgrid composed of two DGUs

Then, by applying the Kirchoff’s current (KCL) and voltage (KVL) laws, the differential equations that describe the dynamic of the i -th node (i.e., DGu_i) are the following

$$\begin{cases} \dot{I}_i = -\frac{R_i}{L_i} I_i - \frac{1}{L_i} V_i + \frac{1}{L_i} U_i \\ \dot{V}_i = \frac{1}{C_i} I_i - \frac{1}{C_i} W_i - \frac{1}{C_i} \sum_{j \in \mathcal{N}_i} I_{ij}, \end{cases} \quad (1)$$

where \mathcal{N}_i is the set of nodes (i.e., DGUs) connected to the i -th node by distribution lines. Moreover, for each $j \in \mathcal{N}_i$, the line dynamics can be expressed as

$$\dot{I}_{ij} = \frac{1}{L_{ij}} (V_i - V_j) - \frac{R_{ij}}{L_{ij}} I_{ij}. \quad (2)$$

Now, we represent the network topology by its corresponding incidence matrix $\mathcal{B} \in \mathbb{R}^{n \times m}$. In particular, one has that

$$\mathcal{B}_{ik} = \begin{cases} +1 & \text{if } I_k \text{ entering into } DGu_i \text{ is assumed positive} \\ -1 & \text{if } I_k \text{ exiting from } DGu_i \text{ is assumed positive} \\ 0 & \text{if } k \text{ is not connected to } i, \end{cases}$$

$I_k = I_{ij}$ being the current exchanged through the edge k (i.e., the line $R_{ij}L_{ij}$) of the graph \mathcal{G} . To study now the overall microgrid we write system (1) and the distribution lines dynamics (2) in a compact way for all the nodes $i \in \mathcal{V}$ as

$$\begin{cases} \dot{I}_t = -L_t^{-1} R_t I_t - L_t^{-1} V + L_t^{-1} U \\ \dot{V} = C_t^{-1} I_t + C_t^{-1} \mathcal{B} I - C_t^{-1} W \\ \dot{I} = -L^{-1} \mathcal{B}^T V - L^{-1} R I, \end{cases} \quad (3)$$

where $V \in \mathbb{R}^n$, $I_t \in \mathbb{R}^n$, $W \in \mathbb{R}^n$, $I \in \mathbb{R}^m$, and $U \in \mathbb{R}^n$ represent, respectively, the following signals: the load voltages, the currents generated by the DGUs, the unknown currents demanded by the loads, the currents along the lines, and the Buck converters output voltages. Moreover C_t , L_t and R_t are $n \times n$ diagonal matrices, while L and R are $m \times m$ diagonal matrices, e.g. $R_t = \text{diag}\{R_{t_1}, \dots, R_{t_n}\}$ and $R = \text{diag}\{R_1, \dots, R_m\}$, with $R_k = R_{ij}$.

3 Problem formulation

Let $x_{[S]}$ denote the vector $[S_1, \dots, S_n]^T$ with $S \in \{V, I_t\}$, and $x_{[I]}$ denote the vector $[I_1, \dots, I_m]^T$, with $I_k = I_{ij}$. Then, system (3) can be written in the so-called state-space representation, i.e.,

$$\begin{cases} \dot{x}_{[I_t]} = -L_t^{-1} R_t x_{[I_t]} - L_t^{-1} x_{[V]} + L_t^{-1} u \\ \dot{x}_{[V]} = C_t^{-1} x_{[I_t]} + C_t^{-1} \mathcal{B} x_{[I]} - C_t^{-1} w \\ \dot{x}_{[I]} = -L^{-1} \mathcal{B}^T x_{[V]} - L^{-1} R x_{[I]} \\ y = x_{[V]}, \end{cases} \quad (4)$$

where $x = [x_{[I_t]}^T x_{[V]}^T x_{[I]}^T]^T \in \mathbb{R}^{2n+m}$ is the state vector, $u = U \in \mathbb{R}^n$ is the control vector, $w = W \in \mathbb{R}^n$ is the disturbance vector, and $y = x_{[V]} \in \mathbb{R}^n$ is the output vector. Then, the previous system can be written in a compact way as

$$\begin{cases} \dot{x} = Ax + Bu + B_w w \\ y = Cx, \end{cases} \quad (5)$$

where $A \in \mathbb{R}^{(2n+m) \times (2n+m)}$ is the dynamics matrix of the microgrid, $B \in \mathbb{R}^{(2n+m) \times n}$, and $B_w \in \mathbb{R}^{(2n+m) \times n}$, and $C \in \mathbb{R}^{n \times (2n+m)}$, as reported above.

To permit the controller design in the next section, the following assumption is required on the state and the disturbance.

Assumption 1 The load voltage V_i is locally available at DGu_i . The disturbance W_i is unknown but bounded and smooth up to the second derivative.

The control problem is now formulated. Let Assumption 1 hold. Given system (1)–(5), design a decentralized control scheme capable of guaranteeing that the tracking error between any controlled variable and the corresponding reference is steered to zero in finite time even in presence of the uncertainties.

4 Proposed control scheme

In this section, a 3-SM control algorithm and a high-gain controller are proposed together with a fuzzy scheduling to solve the aforementioned voltage control problem.

4.1 Third order sliding mode (3-SM) controller

Consider system (5) and select the sliding surface as

$$\sigma = y - y^*, \tag{6}$$

where $\sigma \in \mathbb{R}^n$, and $y^* = x_{[V]}^* \in \mathbb{R}^n$ is the vector of reference values, such that the following assumption is verified.

Assumption 2 Let the references y_i^* , $i = 1, \dots, n$, to have continuous derivative up to order 3.

Moreover, with reference to (6), it appears that the relative degree² is $\rho = 2$, so that a SOSM control naturally applies [40]. In real applications, the discontinuous control can be directly used to open and close the switches of the Buck converters. However, the Insulated Gate Bipolar Transistors (IGBTs) switching frequency cannot be fixed, and then it could be very high, implying the increase of the power losses. Usually, in order to achieve a constant IGBTs switching frequency, Buck converters are controlled by implementing the so-called Pulse Width Modulation (PWM) technique. To do this, a continuous control signal that represents the so-called duty cycle of the Buck converter is required. In order to generate a continuous control signal, as suggested in [40], the system relative degree can be artificially increased. Therefore, by defining the auxiliary variables $\xi_1 = \sigma$, $\xi_2 = \dot{\sigma}$ and $\xi_3 = \ddot{\sigma}$, the auxiliary system can be expressed as

$$\begin{cases} \dot{\xi}_1 = \xi_2 \\ \dot{\xi}_2 = \xi_3 \\ \dot{\xi}_3 = \phi + \Gamma h \\ \dot{u} = h, \end{cases} \tag{7}$$

where ξ_2 and ξ_3 are unmeasurable and

$$\begin{aligned} \phi = & + C_t^{-1} \left(L_t^{-1} R_t L_t^{-1} + \mathcal{B} L^{-1} R L^{-1} \mathcal{B}^T \right) x_{[V]} \\ & + C_t^{-1} \left[L_t^{-1} R_t L_t^{-1} R_t - \left(L_t^{-1} + \mathcal{B} L^{-1} \mathcal{B}^T \right) C_t^{-1} \right] x_{[I]} \\ & + C_t^{-1} \left[\mathcal{B} L^{-1} R L^{-1} R - \left(L_t^{-1} + \mathcal{B} L^{-1} \mathcal{B}^T \right) C_t^{-1} \mathcal{B} \right] x_{[I]} \\ & - C_t^{-1} L_t^{-1} R_t L_t^{-1} u + C_t^{-1} \left(L_t^{-1} + \mathcal{B} L^{-1} \mathcal{B}^T \right) C_t^{-1} w \end{aligned}$$

² The relative degree is the minimum order ρ of the time derivative $\sigma_i^{(\rho)}$, $i = 1, \dots, n$, of the sliding variable associated to the i -th node in which the control u_i , $i = 1, \dots, n$, explicitly appears.

$$\begin{aligned} & - C_t^{-1} \ddot{w} - x_{[V]}^{*(3)}, \\ \Gamma = & C_t^{-1} L_t^{-1} \end{aligned} \tag{8}$$

are uncertain with bounds

$$|\phi_i| \leq \Phi_i, \quad \Gamma_{\min_i} \leq \Gamma_{ii} \leq \Gamma_{\max_i}, \quad i = 1, \dots, n, \tag{9}$$

Φ_i , Γ_{\min_i} and Γ_{\max_i} being known positive constants. Now, the third order Sliding Mode (3-SM) control law proposed in [41] can be used to steer ξ_{1i} , ξ_{2i} and ξ_{3i} , $i=1, \dots, n$, to zero in finite time in spite of the uncertainties, i.e.,

$$h_i = -\alpha_i \begin{cases} h_{1i} = \text{sgn}(\ddot{\sigma}_i), & \bar{\sigma}_i \in M_{1i}/M_{0i} \\ h_{2i} = \text{sgn}\left(\dot{\sigma}_i + \frac{\ddot{\sigma}_i^2 h_{1i}}{2\alpha_{r_i}}\right), & \bar{\sigma}_i \in M_{2i}/M_{1i} \\ h_{3i} = \text{sgn}(s_i(\bar{\sigma}_i)), & \text{else,} \end{cases} \tag{10}$$

with $\bar{\sigma}_i = [\sigma_i, \dot{\sigma}_i, \ddot{\sigma}_i]^T$ and

$$s_i(\bar{\sigma}_i) = \sigma_i + \frac{\ddot{\sigma}_i^3}{3\alpha_{r_i}^2} + h_{2i} \left[\frac{1}{\sqrt{\alpha_{r_i}}} \left(h_{2i} \dot{\sigma}_i + \frac{\ddot{\sigma}_i^2}{2\alpha_{r_i}} \right)^{\frac{3}{2}} + \frac{\dot{\sigma}_i \ddot{\sigma}_i}{\alpha_{r_i}} \right],$$

with

$$\alpha_{r_i} = \alpha_i \Gamma_{\min_i} - \Phi_i > 0. \tag{11}$$

In (10) the manifolds M_{0i} , M_{1i} , M_{2i} are defined as

$$\begin{aligned} M_{0i} &= \{ \bar{\sigma}_i \in \mathbb{R}^3 : \sigma_i = \dot{\sigma}_i = \ddot{\sigma}_i = 0 \} \\ M_{1i} &= \{ \bar{\sigma}_i \in \mathbb{R}^3 : \sigma_i - \frac{\ddot{\sigma}_i^3}{6\alpha_{r_i}^2} = 0, \dot{\sigma}_i + \frac{\ddot{\sigma}_i |\dot{\sigma}_i|}{2\alpha_{r_i}} = 0 \} \\ M_{2i} &= \{ \bar{\sigma}_i \in \mathbb{R}^3 : s_i(\bar{\sigma}_i) = 0 \}. \end{aligned} \tag{12}$$

Note that, in (10) the only parameter to tune is the control amplitude α_i , which is selected according to (11). Moreover, from (7) one can observe that the control signal $h_i = \dot{u}_i$ is discontinuous and affects only $\sigma_i^{(3)}$, while the control actually fed into the plant u_i is continuous. Note that the 3-SM control algorithm is not used to reduce the chattering phenomenon, which is intrinsically generated by the switch of the power converter. The 3-SM control algorithm is applied in order to use the continuous control input u_i as duty cycle of the switch of the i -th Buck converter.

From (10), one can also observe that the controller of DG_{*i*} requires not only σ_i , but also $\dot{\sigma}_i$ and $\ddot{\sigma}_i$. Yet, according to Assumption 1, only the load voltage V_i is measurable at DG_{*i*}. Then, one can rely on Levant's second-order differentiator [42] to retrieve $\dot{\sigma}_i$ and $\ddot{\sigma}_i$ in finite time. With reference to system (7), for $i = 1, \dots, n$, one has

$$\begin{cases} \dot{\hat{\xi}}_{1_i} = -\lambda_{0_i} \left| \hat{\xi}_{1_i} - \xi_{1_i} \right|^{\frac{2}{3}} \operatorname{sgn} \left(\hat{\xi}_{1_i} - \xi_{1_i} \right) + \hat{\xi}_{2_i} \\ \dot{\hat{\xi}}_{2_i} = -\lambda_{1_i} \left| \hat{\xi}_{2_i} - \hat{\xi}_{1_i} \right|^{\frac{1}{2}} \operatorname{sgn} \left(\hat{\xi}_{2_i} - \hat{\xi}_{1_i} \right) + \hat{\xi}_{3_i} \\ \dot{\hat{\xi}}_{3_i} = -\lambda_{2_i} \operatorname{sgn} \left(\hat{\xi}_{3_i} - \hat{\xi}_{2_i} \right), \end{cases} \quad (13)$$

where $\hat{\xi}_{1_i}, \hat{\xi}_{2_i}, \hat{\xi}_{3_i}$ are the estimated values of $\xi_{1_i}, \xi_{2_i}, \xi_{3_i}$, respectively, and $\lambda_{0_i} = 3\Lambda_i^{1/3}, \lambda_{1_i} = 1.5\Lambda_i^{1/2}, \lambda_{2_i} = 1.1\Lambda_i, \Lambda_i > 0$, is a possible choice of the differentiator parameters suggested in [42]. Stability of 3-SM control law (10)–(12) has been shown in [27].

4.2 High-gain controller

The 3-SM controlled presented in Sect. 4.1 has satisfactory performance, including finite-time reaching and strong robustness when the sliding phase is achieved. However, during the reaching phase, especially at the beginning, it is hard to impose limits on the control, hence large control peaks may be necessary. For this reason, in the initial phase it makes sense to use a strategy that limits the control overshoot, like the one proposed in [49]. The following is based on the control strategy presented in [43] and particularized to the case of relative degree two. Preliminarily, the sliding function has to be modified as follows

$$\tilde{\sigma} = \eta - \sigma, \quad \eta = e^{\Sigma t} (c_0 + c_1 t), \quad (14)$$

where Σ is a Hurwitz $n \times n$ real matrix to be suitably selected, while c_0, c_1 are real vectors given by

$$c_0 = y(0) - y^*(0), \quad (15)$$

$$c_1 = \dot{y}(0) - \dot{y}^*(0) - c_0,$$

$y(0), y^*(0), \dot{y}(0), \dot{y}^*(0)$ being the initial conditions of the system output (desired trajectory) and its time derivatives, respectively. Let the control law be defined by the differential equation

$$\begin{aligned} \epsilon^\nu D_\nu u^{(\nu)} + \epsilon^{\nu-1} D_{\nu-1} u^{(\nu-1)} + \dots + \epsilon D_1 \dot{u} \\ = N_2 \ddot{\tilde{\sigma}} + N_1 \dot{\tilde{\sigma}} + N_0 \tilde{\sigma}, \end{aligned} \quad (16)$$

where $\epsilon > 0$ is a “small” real constant, and $D_i, i = 1, \dots, \nu, \nu \geq 2$, and $N_i, i = 0, 1, 2$ are real constant $n \times n$ matrices to be selected as follows:

(i) the matrices N_1, N_2 are such that the algebraic equations

$$N_1 H_1 + N_2 H_2 = M \quad (17)$$

$$N_2 H_1 = 0 \quad (18)$$

are satisfied with M invertible $n \times n$ real matrix;

(ii) the polynomial

$$\det \left(D_\nu s^\nu + D_{\nu-1} s^{\nu-1} + \dots + D_1 s + M \right) \quad (19)$$

is strictly Hurwitz;

(iii) the polynomial

$$\det \left(N_2 s^2 + N_1 s + N_0 \right) \quad (20)$$

is strictly Hurwitz;

iv) the matrix Σ is Hurwitz stable.

Then in this assumptions the stability of control law is guaranteed [43, Theorem 1].

Remark 1 Note that by simple algebraic computations one can show that $H_1 = 0, H_2 = (L_t C_t)^{-1}$, hence condition (i) trivially holds with $N_2 = I$, condition (ii) holds for any diagonal matrices D_1 and D_2 with positive entries, condition (iii) holds for any diagonal matrices N_2, N_1, N_0 with positive entries and any Hurwitz matrix satisfies (iv).

4.3 Fuzzy scheduling

In the previous sections two controllers have been presented. The 3-SM sliding mode controller has satisfactory robustness properties and guarantees sliding mode in finite time. However, in the reaching phase the controlled state may have high overshoot, since there is no focus on the control action limitation. On the contrary, the high-gain controller focuses on the initial transient, thus producing better performances during the reaching phase.

In this section we propose to exploit both strategies, using a fuzzy scheduling of the controllers. The objective is to use the high-gain control during the transient and the 3-SM when the state is closer to the steady-state. The logic we follow is very simple: when the tracking error (i.e., the sliding variable σ) is “small” we use the 3-SM controller, while when the error is “large” the high-gain controller is used. Since the approach to be used in the selection of the appropriate control strategy is simply described in linguistic terms (e.g., steady-state, selection of the “stronger” control action during transient) a natural candidate scheduler is a fuzzy one. This approach has the added value of producing simply an overall control action that is continuous. The idea of using fuzzy inference systems (FIS) as scheduler among different controllers is not new [50–52]. As it is well-known, the advantage of using a fuzzy scheduling strategy (as opposite to any other switching strategy) is that fuzzy scheduler produces smooth signals.

A Sugeno FIS has been designed, with the tracking error as input and the selected control as output. The set of membership functions (MFs) we use is very simple: just three MFs,

namely, transient-NEG and transient-POS for transient negative or positive error, respectively, and Steadystate, when the state can be considered in steady state (i.e., when the tracking error is “small”).

Relying on the above MFs, a preliminary version of the switching strategy, employing only two simple rules, is formulated.

- if (σ is transient-NEG) or (σ is transient-POS) then $u = u_{hg}$,
- if (σ is Steadystate) then $u = u_s$,

where u_{hg} and u_s are the control actions generated by the high-gain and by the 3-SM controllers, respectively.

The above strategy is very simple, and assumes that the control will start with the high-gain strategy, ending with the sliding mode control. However, a corrective action is in order. During the initial transient the actual control follows the high-gain strategy although the SM controller is active (but ineffective in controlling the system, since the SM control is overrun by the fuzzy scheduler). Then the sliding mode controller “sees” a discrepancy between its commanded action and the plant evolution. This discrepancy is obviously interpreted as a disturbance, thus the sliding mode controller can produce large control values to compensate for this fictitious disturbance. This makes no harm until the high gain strategy is selected. However, when the tracking error is reduced, the control goes towards the values required by the sliding controller, that can be now very large, thus an overshoot could occur in the control. The phenomenon is in some sense similar to the well-known “wind-up” of the integral controllers. In order to avoid this phenomenon, it is possible to add two rules such that if the absolute value of the control generated by the sliding mode action is larger than the one required by

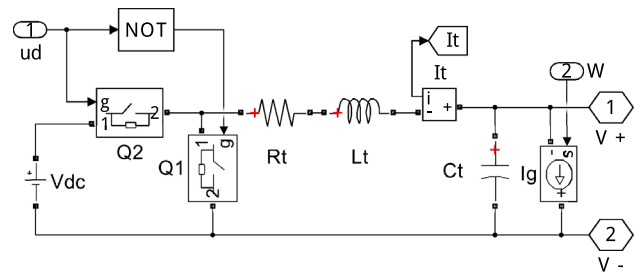


Fig. 3 Simulink scheme of a DGU

the high-gain, then the control must follow the sliding mode control law.

Combining together the rules, the following rule-base is obtained.

- if (σ is transient-NEG) or (σ is transient-POS) then $u = u_{hg}$,
- if (σ is Steadystate) then $u = u_s$,
- if (δ_u is POS) then $u = u_s$,
- if (δ_u is NEG) then $u = u_{hg}$,

where $\delta_u = |u_s| - |u_{hg}|$, and NEG, POS are two MFs expressing “negative” and “positive”, respectively. Note that the third and the fourth rule in some sense contradict the first two, since they select the *largest* control action. One of the advantages of the use of fuzzy logic-based scheduling controllers is exactly the possibility to use rules in apparent contradiction, since the true “firing strength” of each rule depends nonlinearly on the system behaviour. In other words, by suitably choosing the fuzzy scheduler parameters it is possible that the first two rules will dominate at the beginning (during the reaching phase), while the effect of the last two rules will be apparent in a proximity of the sliding manifold.

Fig. 2 Simulink scheme of controlled DC microgrid

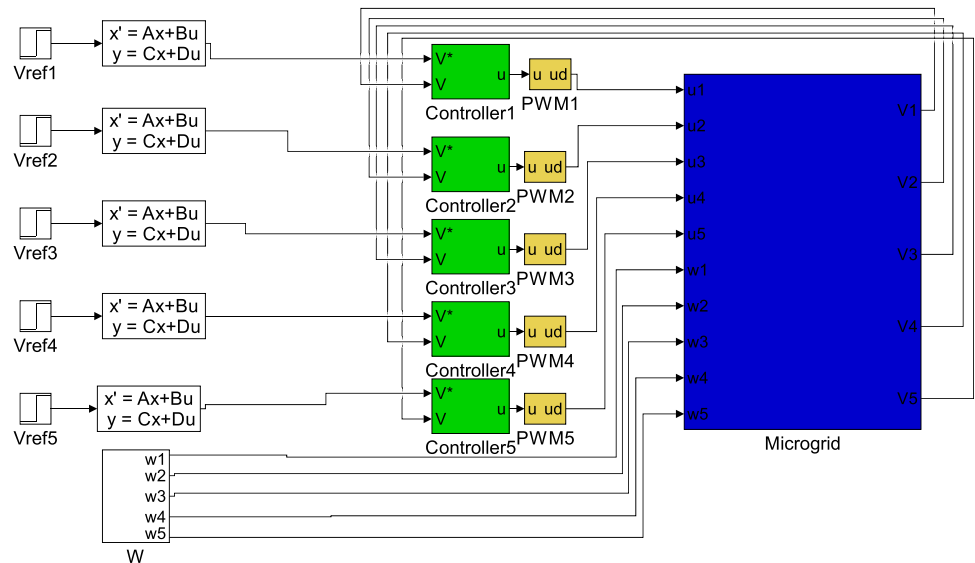


Fig. 4 Simulink scheme of the considered microgrid

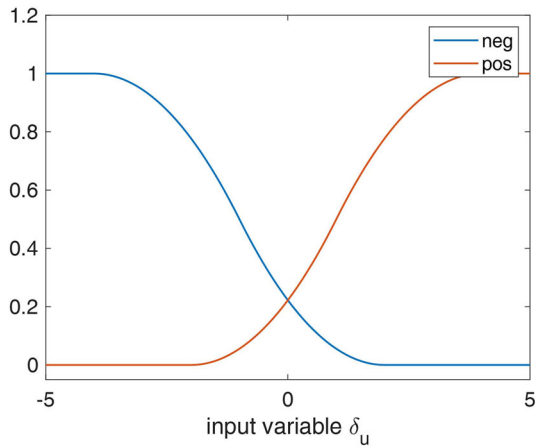
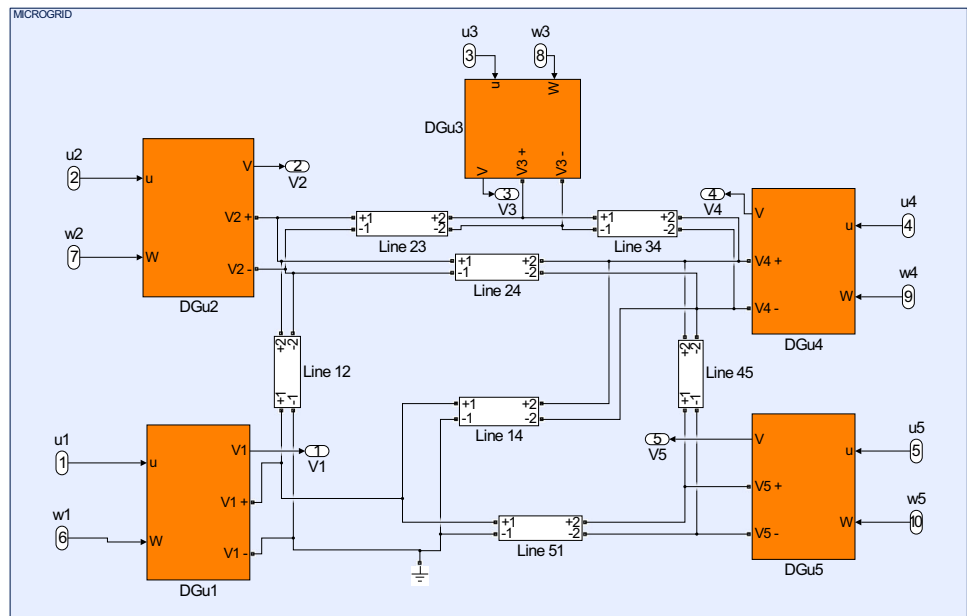


Fig. 5 Membership function of δ_u

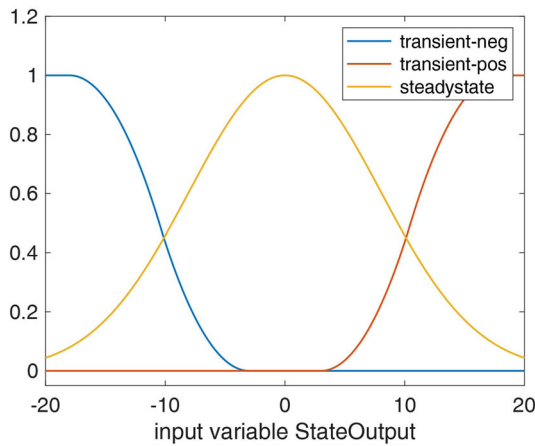


Fig. 6 Membership function for identification of transient or steady state

Table 1 Rules of fuzzy block

Rule 1	$StateOutput$ is transient-neg or transient-pos	output is u_{hg}
Rule 2	$StateOutput$ is SteadyState	output is u_s
Rule 3	δ_u is positive	output is u_s
Rule 4	δ_u is negative	output is u_{hg}

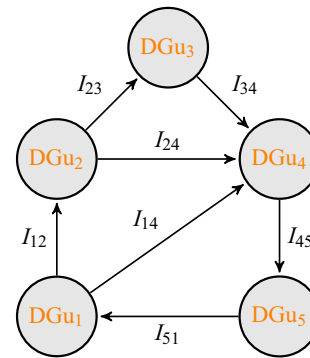


Fig. 7 Block diagram of the connections of DGus. The arrows indicate the positive direction of the currents through the power network

Table 2 Buck filter parameters

	R_f (Ω)	L_f (mH)	C_f (mF)
DGu ₁	0.2	1.8	2
DGu ₂	0.1	1.6	2.1
DGu ₃	0.3	2	1.8
DGu ₄	0.4	2.1	1.9
DGu ₅	0.5	1.9	2.2

Table 3 Line parameters

	R (m Ω)	L (μ H)
Line ₁₂	50	1.9
Line ₁₄	60	2
Line ₂₃	40	1.7
Line ₂₄	80	2.1
Line ₃₄	70	1.8
Line ₄₅	65	1.6
Line ₅₁	45	2

Table 4 Loads and voltage references

	W_i (A)	t (s)	ΔW_i (A)	V_i^* (V)	t (s)	ΔV_i^* (V)
DGu ₁	20	11	- 10	380	0.2	+ 0.5
DGu ₂	10	12	+ 10	380	-	-
DGu ₃	15	13	+ 15	380	0.3	- 0.5
DGu ₄	30	14	- 15	380	-	-
DGu ₅	5	14	+ 20	380	0.4	- 0.5

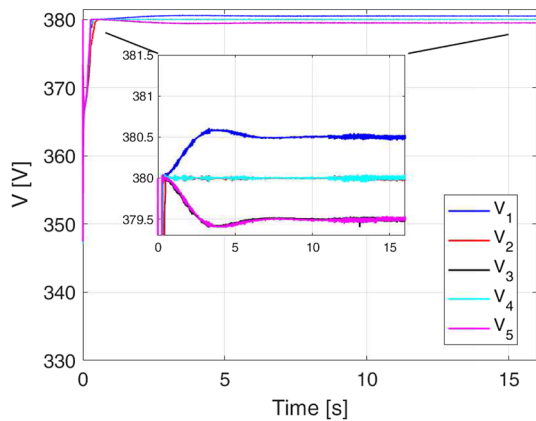


Fig. 8 Load voltages

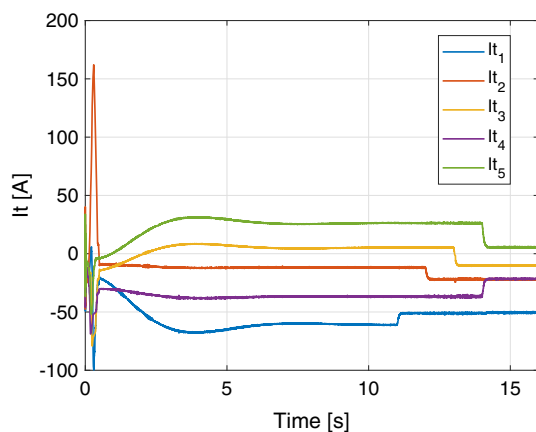


Fig. 9 Generated currents (at the output of the $L_i C_i$ filter of the converter)

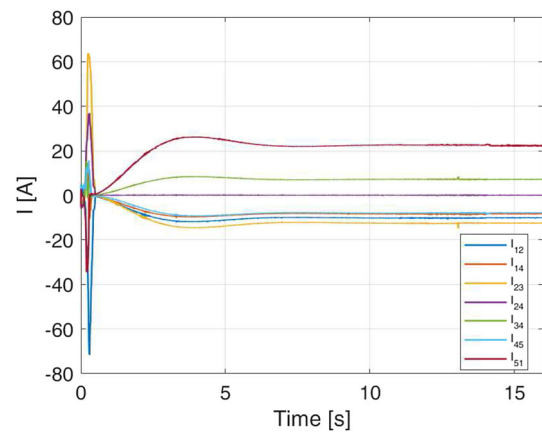


Fig. 10 The currents through the distribution lines

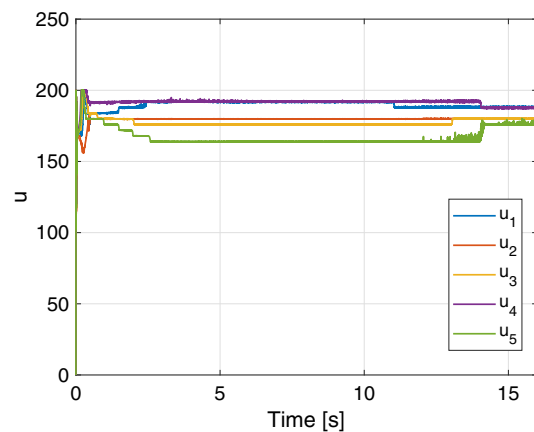


Fig. 11 Controlled buck converter output voltage

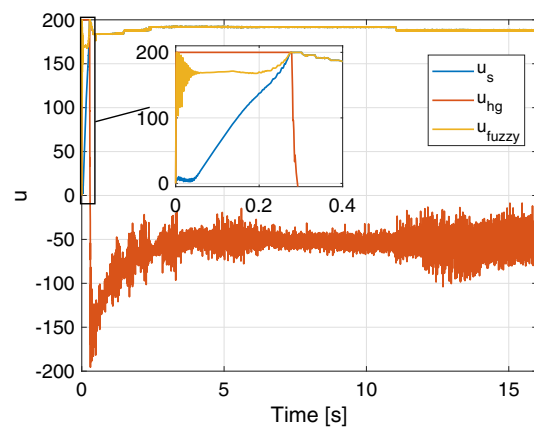


Fig. 12 Comparison between the controllers K_s , K_{hg} of DGu₁ without fuzzy control, and the selected control with fuzzy scheduling

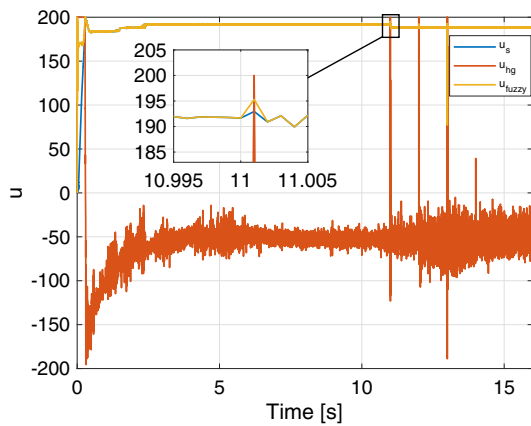


Fig. 13 Comparison between K_s , K_{hg} of DG_{U1} w/o fuzzy control, and the selected control with fuzzy scheduling, step-wise changing loads

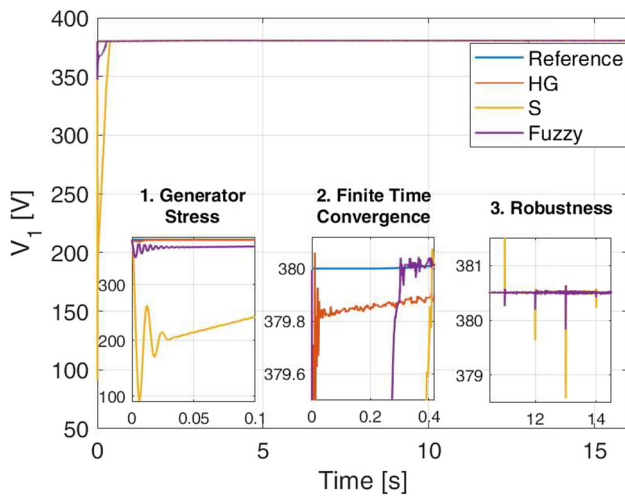


Fig. 14 Comparison of the effect of different controllers on the first load voltage, step-wise changing loads

The tuning of the five MFs has been done heuristically, but it is possible also to use nonlinear optimization algorithms in order to automate the tuning procedure.

5 Simulation results

In order to test the proposed strategy a MATLAB/Simulink/SimPowerSystem simulator has been implemented as shown in Fig. 2. Each DGU has been implemented with a Buck converter, as shown in Fig. 3. The block (blue) Microgrid is a realistic network of 5 DGUs as shown in Fig. 4. In the green blocks there are

- Third order sliding mode controller (K_s) in (10)–(12).
- High gain controller (K_{hg}) in (16).
- Fuzzy controller logic, that switch between the controllers K_s and K_{hg} according with the membership functions in Figs. 5 and 6, and rules in Table 1.

The MF parameters have been initially selected heuristically, and then a fine-tuning of the parameters has been carried out by using a Genetic Optimiser on a simplified version of the simulator (simplified removing the switching behaviour and replacing the model with an average model). In order to simplify computation, symmetry of the MFs around zero has been imposed, and only 20 generations have been used, since any increase in the number of generations has produced no meaningful improvement.

The microgrid connection can be described by a Block Diagram, as depicted in Fig. 7, and using the following incidence matrix $B \in \mathbb{R}^{5 \times 7}$

$$B = \begin{bmatrix} -1 & -1 & 0 & 0 & 0 & 0 & 1 \\ 1 & 0 & -1 & -1 & 0 & 0 & 0 \\ 0 & 0 & 1 & 0 & -1 & 0 & 0 \\ 0 & 1 & 0 & 1 & 1 & -1 & 0 \\ 0 & 0 & 0 & 0 & 0 & 1 & -1 \end{bmatrix}.$$

The electrical parameters considered in simulation are given in Tables 2 and 3. For the high gain controller note that, by using (4), the parameters in (16) are $H_1 = 0$ and $H_2 = (L_t C_t)^{-1}$, hence (18) trivially holds, while by selecting, for the sake of simplicity, N_i and D_i as diagonal matrices with positive entries all the hypothesis of Sect. 4.2 hold. The control parameters of K_s and K_{hg} are $\alpha = 2.5 \cdot 10^3$, $\Sigma = 1000I$, $\nu = 2$, $\epsilon = 0.001$, $D_1 = I$, $D_2 = I$, $N_0 = I$, $N_1 = 2I$ $N_2 = 1.1I$ (I being the 5×5 identity matrix). In order to test the proposed control scheme, the loads and the voltage references change according to Table 4.

Note that the variations are such that the Assumptions 1 and 2 are verified. Figure 8 shows the time evolution of the load voltages, and one can note that the proposed controllers track very well the voltage references of all DGUs. Moreover, in Figs. 9 and 10 the generated currents and the currents through the distribution lines are reported, respectively. Finally, Fig. 11 shows the time evolution of the control inputs u_i , with $i = 1, \dots, 5$. In particular, Fig. 12 puts into evidence the output control signal generated by K_s , K_{hg} and Fuzzy Logic, respectively. Before 0.2 s the fuzzy chooses the high gain controller, instead when the control of K_s is higher, it instantly changes control strategy.

Up to now, we have supposed Assumptions 1 and 2 to hold. Although it is reasonable to consider the load to change smoothly, a critical situation can happen if the variation of some loads is very fast. In order to face this issue, we assume the worst-case scenario considering stepwise changing loads. The numerical values for the loads are still those in Table 4. In this case the 3-SM controller is unable to keep the system state on the manifold after the commutation, and a new reaching phase would take place. At this point the fuzzy scheduler commutes again to the HG controller, as at the very initial phase. This is apparent in Fig. 13, that is basically the same as

Fig. 12, but it is clear that in case of abrupt load commutation the control is a fuzzy mixture of HG and 3-SM controllers.

The key points of the proposed strategy are illustrated in Fig. 14, where the usage of different control strategies on the voltage V_1 is shown. Specifically, it is apparent that the fuzzy controller alleviates the initial generator stress (and actually the generator stress at any sudden load change). On the other side, the fuzzy controller inherits a finite-time convergence capability from the 3-SM controller. Finally, if the load is seen as a disturbance, the strong disturbance rejection property of the HG approach reflects into the fuzzy controller.

6 Conclusions

In this paper a decentralized control scheme based on Sliding Mode control strategies is designed to regulate the voltage in islanded buck-based DC microgrids with arbitrary complex topology. The model of a DC buck-based microgrid composed of several interconnected Distributed Generation Units through power lines is introduced by using a connected and undirected graph to represent power network. In particular, a mixed strategy, employing both a third-order sliding mode control algorithm and a high gain control strategy with a fuzzy scheduling. The chattering alleviation performed by the 3-SM control algorithm allows one to obtain a continuous control signal that can be used in PWM technique as duty cycle of the switch of the Buck converter in order to attain a constant switching frequency. The asymptotic stability of the whole system is proved, and the performance of the proposed decentralized control approach is evaluated in simulation considering a DC microgrid composed of five DGUs arranged in a meshed topology including loops. Moreover the mixed approach allows to have a less generator stress, a finite time convergence and a more robustness. Finally a simulation scenario is presented to show the effectiveness and the advantage of the proposed strategy. The future works will address on a supervisory strategy rather than a fuzzy approach, in order to understand the best methodology to use both controllers. Moreover, the experimental results will be an important point to improve the importance of this mixed control.

References

- Ackermann T, Andersson G, Söder L (2001) Distributed generation: a definition. *Electr Power Syst Res* 57(3):195–204
- Pepermans G, Driesen J, Haeseldonckx D, Belmans R, D'haeseleer W (2005) Distributed generation: definition, benefits and issues. *Energy Policy* 33(6):787–798
- Blaabjerg F, Teodorescu R, Liserre M, Timbus AV (2006) Overview of control and grid synchronization for distributed power generation systems. *IEEE Trans Ind Electron* 53(5):1398–1409
- Carrasco JM, Franquelo LG, Bialasiewicz JT, Galvan E, PortilloGuisado RC, Prats MAM, Leon JI, Moreno-Alfonso N (2006) Power-electronic systems for the grid integration of renewable energy sources: a survey. *IEEE Trans Ind Electron* 53(4):1002–1016
- Liserre M, Sauter T, Hung JY (2010) Future energy systems: integrating renewable energy sources into the smart power grid through industrial electronics. *IEEE Ind Electron Mag* 4(1):18–37
- Katiraei F, Iravani MR (2006) Power management strategies for a microgrid with multiple distributed generation units. *IEEE Trans Power Syst* 21(4):1821–1831
- Farhangi H (2010) The path of the smart grid. *IEEE Power Energy Mag* 8(1):18–28
- Hatziargyriou N, Asano H, Iravani R, Marnay C (2007) Microgrids. *IEEE Power Energy Mag* 5(4):78–94
- Lasseter R (2002) Microgrids. In: *IEEE power engineering society winter meeting*, vol 1, pp 305–308
- Lasseter R, Paigi P (2004) Microgrid: a conceptual solution. In: *Proc. 35th IEEE power electron. specialists conf., Aachen*, vol 6, pp 4285–4290
- Katiraei F, Iravani M, Lehn P (2005) Micro-grid autonomous operation during and subsequent to islanding process. *IEEE Trans Power Deliv* 20(1):248–257
- Lopes JAP, Moreira CL, Madureira AG (2006) Defining control strategies for microgrids islanded operation. *IEEE Trans Power Syst* 21(2):916–924
- Guerrero JM, Chandorkar M, Lee T-L, Loh PC (2013) Advanced control architectures for intelligent microgrids, part i: decentralized and hierarchical control. *IEEE Trans Ind Electron* 60(4):1254–1262
- Sadabadi MS, Shafiee Q, Karimi A (2016) Plug-and-play voltage stabilization in inverter-interfaced microgrids via a robust control strategy. *IEEE Trans Control Syst Technol* 24(1):1–11
- Cucuzzella M, Incremona GP, Ferrara A (2015) Design of robust higher order sliding mode control for microgrids. *IEEE J Emerg Sel Topics Circuits Syst* 5(3):393–401
- Incremona GP, Cucuzzella M, Ferrara A (2016) Adaptive suboptimal second-order sliding mode control for microgrids. *Int J Control* 89(9):1849–1867
- Cucuzzella M, Incremona GP, Ferrara A (2017) Decentralized sliding mode control of islanded ac microgrids with arbitrary topology. *IEEE Trans Ind Electron* 64(8):6706–6713
- Guida B, Cavallo A (2012) Supervised bidirectional dc/dc converter for intelligent fuel cell vehicles energy management. In: *Electric Vehicle Conference (IEVC), 2012 IEEE International*. IEEE, pp 1–5
- Canciello G, Cavallo A, Guida B (2017) Control of energy storage systems for aeronautic applications. *J Control Sci Eng* 2017:2458590
- Canciello G, Cavallo A, Guida B (2017) Robust control of aeronautical electrical generators for energy management applications. *Int J Aerosp Eng* 2017:1745154
- Canciello G, Russo A, Guida B, Cavallo A (2018) Supervisory control for energy storage system onboard aircraft. In: *2018 IEEE international conference on environment and electrical engineering and 2018 IEEE industrial and commercial power systems Europe (EEEIC/I&CPS Europe)*. IEEE, pp 1–6
- Guida B, Cavallo A (2013) A petri net application for energy management in aeronautical networks. In: *Emerging Technologies & Factory Automation (ETFA), 2013 IEEE 18th Conference on*. IEEE, pp 1–6
- Guerrero JM, Vasquez JC, Matas J, de Vicuna LG, Castilla M (2011) Hierarchical control of droop-controlled ac and dc microgrids—a general approach toward standardization. *IEEE Trans Ind Electron* 58(1):158–172

24. Justo JJ, Mwasilu F, Lee J, Jung J-W (2013) Ac-microgrids versus dc-microgrids with distributed energy resources: a review. *Renew Sustain Energy Rev* 24:387–405
25. Rodriguez-Diaz E, Savaghebi M, Vasquez JC, Guerrero JM (2015) An overview of low voltage dc distribution systems for residential applications. In: 2015 IEEE 5th international conference on Consumer electronics—Berlin (ICCE-Berlin), pp 318–322
26. Guida B, Rubino L, Marino P, Cavallo A (2010) Implementation of control and protection logics for a bidirectional dc/dc converter. In: *Industrial Electronics (ISIE), 2010 IEEE International Symposium on*. IEEE. pp 2696–2701
27. Cucuzzella M, Rosti S, Cavallo A, Ferrara A (2017) Decentralized sliding mode voltage control in dc microgrids. In: *Proc. American control conf, Seattle*
28. Cucuzzella M, Lazzari R, Trip S, Rosti S, Sandroni C, Ferrara A (2018) Sliding mode voltage control of boost converters in DC microgrids. *Control Eng Pract* 73:161–170
29. Ferreira RAF, Braga HAC, Ferreira AA, Barbosa PG (2012) Analysis of voltage droop control method for dc microgrids with simulink: modelling and simulation. In: 2012 10th IEEE/IAS international conference on industry applications (INDUSCON), pp 1–6
30. Cucuzzella M, Trip S, De Persis C, Cheng X, Ferrara A, van der Schaft A (2018) A robust consensus algorithm for current sharing and voltage regulation in DC microgrids. *IEEE Trans Control Syst Technol*. <https://doi.org/10.1109/TCST.2018.2834878>
31. Trip S, Cucuzzella M, Cheng X, Scherpen J (2019) Distributed averaging control for voltage regulation and current sharing in DC microgrids. *IEEE Control Syst Lett* 3(1):174–179
32. Chen YK, Wu YC, Song CC, Chen YS (2013) Design and implementation of energy management system with fuzzy control for dc microgrid systems. *IEEE Trans Power Electron* 28(4):1563–1570
33. Kakigano H, Miura Y, Ise T (2013) Distribution voltage control for dc microgrids using fuzzy control and gain-scheduling technique. *IEEE Trans Power Electron* 28(5):2246–2258
34. Shadmand MB, Balog RS, Abu-Rub H (2014) Model predictive control of pv sources in a smart dc distribution system: maximum power point tracking and droop control. *IEEE Trans Energy Convers* 29(4):913–921
35. Utkin VI (1992) *Sliding modes in optimization and control problems*. Springer, New York
36. Edwards C, Spurgeon SK (1998) *Sliding mode control: theory and applications*. Taylor and Francis, London
37. Tan S-C, Lai YM, Cheung MKH, Tse CK (2005) On the practical design of a sliding mode voltage controlled buck converter. *IEEE Trans Power Electron* 20(2):425–437
38. Mahdavi J, Emadi A, Toliyat HA (1997) Application of state space averaging method to sliding mode control of pwm dc/dc converters. In: *Industry applications conference, 1997. Thirty-second IAS annual meeting, IAS '97., Conference record of the 1997 IEEE, vol 2*, pp 820–827
39. Spiazzi G, Mattavelli P, Rossetto L (1997) Sliding mode control of dc–dc converters. *System* 2:1
40. Bartolini G, Ferrara A, Usai E (1998) Chattering avoidance by second-order sliding mode control. *IEEE Trans Autom Control* 43(2):241–246
41. Dinuzzo F, Ferrara A (2009) Higher order sliding mode controllers with optimal reaching. *IEEE Trans Autom Control* 54(9):2126–2136
42. Levant A (2003) Higher-order sliding modes, differentiation and output-feedback control. *Int J Control* 76(9–10):924–941
43. Cavallo A, Natale C (2003) Output feedback control based on a high-order sliding manifold approach. *IEEE Trans Autom Control* 48(3):469–472
44. Cavallo A, Canciello G, Guida B (2017) Supervisory control of dc–dc bidirectional converter for advanced aeronautic applications. *Int J Robust Nonlinear Control*. <http://dx.doi.org/10.1002/rnc.3851>
45. Cavallo A, Canciello G, Guida B, Kulsangcharoen P, Yeoh S, Rashed M, Bozhko S (2018) Multi-objective supervisory control for dc/dc converters in advanced aeronautic applications. *Energies* 11(11):3216
46. Cavallo A, Canciello G, Guida B (2017) Energy storage system control for energy management in advanced aeronautic applications. *Math Probl Eng* 2017:4083132
47. Cavallo A, Guida B, Buonanno A, Sparaco E (2015) Smart buck-boost converter unit operations for aeronautical applications. In: 54rd IEEE conference on decision and control, CDC 2015, pp 4734–4739
48. Cavallo A, Canciello G, Guida B (2017) Supervised control of buck-boost converters for aeronautical applications. *Automatica* 83:73–80
49. Cavallo A, de Maria G, Nistri P (1999) Robust control design with integral action and limited rate control. *IEEE Trans Autom Control* 44(8):1569–1572
50. Fahmy M (2010) A fuzzy algorithm for scheduling non-periodic jobs on soft real-time single processor system. *Ain Shams Eng J* 1(1):31–38
51. Plius MP, Yilmaz M, Seven U, Erbatır K (2012) Fuzzy controller scheduling for robotic manipulator force control. In: 2012 12th IEEE international workshop on advanced motion control (AMC), pp 1–8
52. Syed FU, Kuang ML, Smith M, Okubo S, Ying H (2009) Fuzzy gain-scheduling proportional-integral control for improving engine power and speed behavior in a hybrid electric vehicle. *IEEE Trans Veh Technol* 58(1):69–84